

THE POSSIBILITIES OF THE LASER MODIFICATION OF THE MALLEABLE IRON SURFACE

Summary

The aim of the presented investigation was to perform surface modification of the malleable iron by laser alloying and evaluate the influence of the laser heat treatment (LHT) on the microstructure of its surface layer (particularly in comparison to the other gray irons). After LHT of the malleable iron modified microstructure of its surface layer with very fine-crystalline, homogenous and hard ($>1000\text{HV}0.1$) melted zone was achieved. 4-fold increased hardness (in comparison to the hardness of matrix of the core material) of melted zone resulted not only from very fine and hardened microstructure, but also due to supersaturating with alloying elements. Gentle hardness changes on the cross section of the surface layer from the melted zone to the core material was noticed. The depth of melted zone was approx. 0.7 mm and it corresponded to the counted depth. It was stated that due to malleable iron specific thermophysical properties smaller depth of modified layer than achieved depth for flake irons and much smaller than the depth for nodular irons for the same LHT conditions could be expected.

Key words: laser heat treatment, malleable iron, thermophysical properties

MOŻLIWOŚCI LASEROWEJ MODYFIKACJI POWIERZCHNI ŻELIWA CIĄGLIWEGO

Streszczenie

Celem prezentowanych badań było przeprowadzenie obróbki powierzchniowej żeliwa ciągliwego przez stopowanie laserowe oraz ocena wpływu laserowej obróbki cieplnej (LOC) na mikrostrukturę jego warstwy wierzchniej (w szczególności w porównaniu do innych żeliw szarych). Po LOC żeliwa ciągliwego uzyskano mikrostrukturę jego warstwy wierzchniej z drobnokrystaliczną, jednorodną i twardą ($>1000\text{HV}0.1$) strefą przetopioną. 4-krotne zwiększenie twardości (w porównaniu do twardości osnowy materiału rdzenia) strefy przetopionej nie wynikała tylko z bardzo drobnej i zahartowanej mikrostruktury, ale również z przesylenia wprowadzonymi pierwiastkami stopowymi. Zaobserwowano łagodną zmianę twardości na przekroju poprzecznym od strefy przetopionej do rdzenia. Głębokość strefy przetopionej wynosiła około 0.7 mm i była zbliżona do wartości obliczonej. Stwierdzono, że w wyniku specyficznych właściwości termofizycznych żeliwa ciągliwego można się spodziewać osiągnięcia mniejszej głębokości warstwy zmodyfikowanej niż w przypadku głębokości dla żeliw płatkowych i o wiele mniejszej niż w przypadku żeliw sferoidalnych (uzyskanej w tych samych warunkach LOC).

Słowa kluczowe: laserowa obróbka cieplna, żeliwo ciągliwe, właściwości termofizyczne

1. Introduction

The design and production of agricultural machines is the one of the most important trend in case of enhancement of the agricultural technique. Selection of appropriate material with adequate hardness and wear resistance are important from the point of view of the exploitation of agricultural and heavy duty machinery, especially for components of machines that work in the soil [1]. Furthermore, application of new materials and their modern production methods could cause significant changes in the construction of machines. These methods include surface treatments dedicated to parts especially exposed to wear and/or corrosion [2]. One of these methods consists in laser heat treatment (LHT) that allows to improve materials surface layer microstructure and properties. Gray irons are very popular group of materials. They are used in automotive branch (like crankshafts, camshafts) [3], rail industry (breaking discs) [4], etc. Gray irons are also common in case of agricultural machines. Modified gray irons as: nodular, vermicular and malleable with superior (than flake irons) mechanical properties are particularly interesting. For example, nodular iron, after appropriate treatment could replace cast steel or even steel in some parts of machines. As the re-

search (presented in [5, 6]) showed, for instance, 38GSA steel usually used for functioning plough blades in soil could be replaced by ADI cast iron.

It needs to be taken into account that some parts of agricultural machines (made of cast irons) like: shafts of harvest machine, gears, teeth harrows, disc harrows, coulter presser feet are exposed to tribological wear.

The study presented in this article concerns laser surface treatment that might be used in case of devices made of malleable iron. The previous own research [7] showed that it is possible to implement boron and silicon (or with boron, silicon and cobalt as well) into the surface layer of EN-GJL-250 flake iron with pearlite matrix and EN-GJS-600-3 nodular iron with ferrite-pearlite matrix by laser alloying. The alloying zone with boron and silicon was characterized by ultra-fine microstructure with hardness in the range of 1200–1700 HV0.1 (depending on the value of the laser beam parameters) which could improve the durability and reliability of the particular machine part. Such result creates great possibilities to widen the application of many kinds of gray iron.

In order to achieve particular effect in the surface layer of the treated material an appropriate laser heat treatment parameter selection is needed [8]. One of the most im-

portant aspects that should be taken into account in this section are thermophysical properties of treated material. The comparison of those properties of different gray irons is presented in [9]. Malleable iron is characterized by higher density ($7.3 \text{ g}\cdot\text{cm}^{-2}$) than most of flake or nodular irons ($7.1 \text{ g}\cdot\text{cm}^{-2}$). Its specific heat is $523\text{-}527 \text{ J}\cdot\text{kg}^{-1}\cdot\text{K}^{-1}$, while for most of gray irons is rather below $500 \text{ J}\cdot\text{kg}^{-1}\cdot\text{K}^{-1}$. Thermal conductivity of malleable iron is $50.2\text{-}54.4 \text{ W}\cdot\text{m}^{-1}\cdot\text{K}^{-1}$ – similar to flake irons. This makes that some surface effects of LHT could be different in case of this iron than the rest [9].

The aim of the presented research was to perform the malleable iron modification by laser alloying and evaluate the influence of the laser heat treatment on the microstructure of the surface layer (especially in comparison to the other gray irons). This study is a part of the research on LHT application to gray iron. The general purpose of this research is improving the useful properties of machine part made of gray iron.

2. Methodology

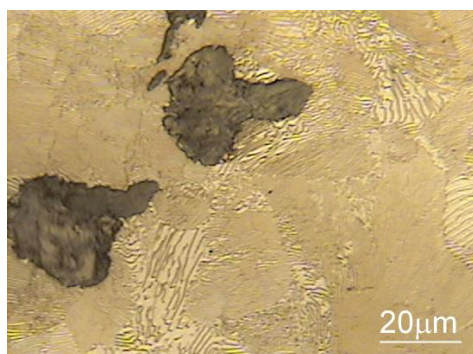
Blackheart malleable cast iron EN-GJMB-450-6 with pearlite matrix was chosen as the test material. This cast iron was characterized by average hardness of 20 HRC (with 270 HV0.1 hardness of the matrix). The graphite and pearlite in the investigated malleable iron was presented in the Fig. 1. The chemical composition of investigated iron was shown in Table 1.

Table 1. The chemical composition of the EN-GJMB-450-6 malleable iron

Tab. 1. Skład chemiczny żeliwa ciągliwego EN-GJMB-450-6

Cast iron	The element value % [wt.]						
	C	Si	Mn	P	S	Cr	Cu
EN-GJMB-450-6	2.30	1.2	0.59	0.03	0.013	0.08	0.03

Source: own work / Źródło: opracowanie własne



Source: own work / Źródło: opracowanie własne

Fig. 1. The microstructure of the EN-GJMB-450-6 malleable iron. Etched with nitride acid solution
Rys. 1. Mikrostruktura żeliwa ciągliwego EN-GJMB-450-6. Trawione nitalem

Laser heat treatment consisted in laser heating of the surface layer of sample made of tested cast iron. The aim of heating was to achieve the melting of the part of the surface layer. Molecular CO₂ continuous Trumpf laser type TLF 2600T with 2.6-kW output power and TEM0.1 mode was used. As mentioned in the introduction of this paper malleable iron is characterized by specific thermophysical properties. Its specific heat is in about 10% higher than specific heat of flake or nodular iron. Malleable iron is character-

ized by much smaller amount of carbon than those cast irons (that usually possess about 3.5%) and higher density. These properties need to be taken into account during laser beam parameters selection. On the base of own research on different cast irons and equations proposed by Ashby and Esterling [10] allowing to predict the values of temperatures and cooling rates laser heat treatment parameters were selected. The evaluation of the temperature changes on the section of the sample is important to assess the expected depth of remelted zone in the surface layer in the laser treated material. Thus, to calculate the temperature following equation was applied [10]:

$$T(y, z, t) = T_0 + \frac{A \cdot P}{2 \cdot \pi \cdot \lambda \cdot v \cdot [t(t+t_0)]^{\frac{1}{2}}} \cdot \exp\left\{-\left[\frac{(z+z_0)^2}{4 \cdot \alpha \cdot t} + \frac{y^2}{4 \cdot \alpha(t+t_0)}\right]\right\}; \quad (1)$$

where: $T(y, z, t)$ – temperature [K] at (y, z) ; y, z – coordinates [m]; T_0 – ambient temperature [K]; A – absorptivity [%]; P – laser beam power [W]; λ – material thermal conductivity [$\text{W}\cdot\text{m}^{-1}\cdot\text{K}^{-1}$]; v – laser beam velocity [$\text{m}\cdot\text{s}^{-1}$]; t – interaction time [s], t_0 – variable, represents the time required for heat to diffuse over a distance equal to the beam radius on the sample surface:

$$t_0 = \frac{r^2}{4 \cdot \alpha}; \quad (2)$$

where: r – laser beam radius [m]; α – thermal diffusivity [$\text{m}^2\cdot\text{s}^{-1}$]; z_0 – variable, measures the distance over which heat can diffuse during the laser beam interaction time.

If $t \gg t_0$ (like in this case), z_0 can be expressed by the equation:

$$z_0 = \frac{r^{\frac{1}{2}}}{e} \cdot \left(\frac{\pi \cdot \alpha \cdot r}{v}\right)^{\frac{1}{4}}; \quad (3)$$

and the maximum temperature can be assessed using following equation:

$$T_{\max} = T_0 + \frac{2 \cdot A \cdot P}{\pi \cdot e \cdot \rho \cdot C_p \cdot v \cdot (z+z_0)^2}; \quad (4)$$

where: ρ – material density [$\text{kg}\cdot\text{m}^{-3}$]; C_p – material specific heat [$\text{J}\cdot\text{kg}^{-1}\cdot\text{K}^{-1}$].

Warming and cooling rate can be estimated by means of equation:

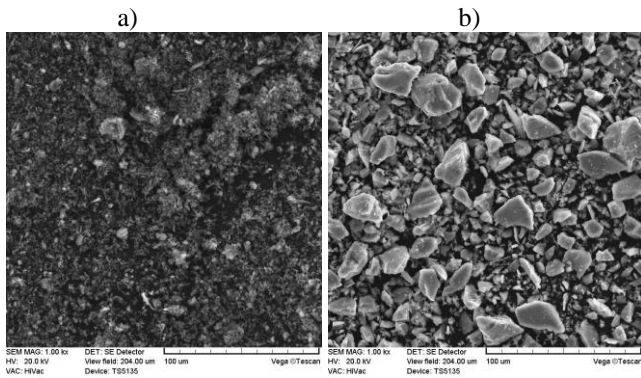
$$\frac{\Delta T}{\Delta t} = \frac{T_{\max} - T_0}{t} \left[\frac{(z+z_0)^2}{4 \cdot \alpha \cdot t} - \frac{1}{2} \left(\frac{2t+t_0}{t+t_0} \right) \right]; \quad (5)$$

where the first part in the square bracket represents heating, and the second one describes cooling. Laser beam parameters were chosen to achieve such temperature in the surface layer which would cause remelting. Laser beam power density E was $26 \text{ W}\cdot\text{mm}^{-2}$ and its scanning velocity V was $1.87 \text{ mm}\cdot\text{s}^{-1}$.

Due to good results achieved in case of flake and nodular irons with alloying them with boron and silicon before laser heating the sample of malleable iron was also covered with the paste containing such alloying substance (the powder of amorphous boron and silicon – Fig. 2) and a bonding substance (the water glass). Size of the particle in case of boron was $<1 \mu\text{m}$ and 325 mesh for silicon. Their purities were: $\geq 95\%$ for boron and 99% for silicon. Laser beam caused simultaneously melting of the alloying substance with thin layer of covered material. Then, those melted materials were mixed and rapidly cooled. As a result, a new

alloy, different from material of malleable iron and paste containing boron and silicon, was created.

The laser heat treatment results were analyzed by means of optical microscope (microstructure evaluation and modified zones determination) and Vickers hardness tester with 100G of load (microhardness distribution on the section). The investigation was performed at the Institute of Machines and Motor Vehicle, Poznan University of Technology.

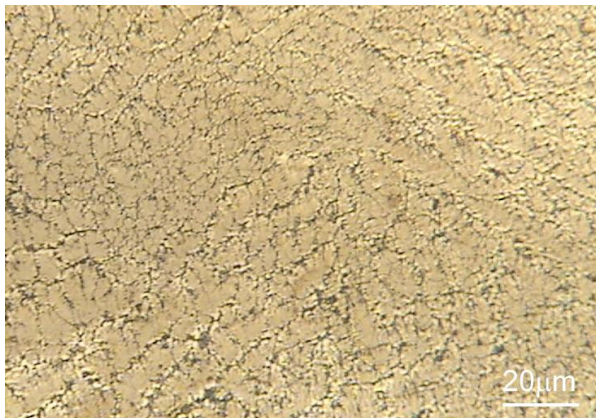


Source: own work / Źródło: opracowanie własne

Fig. 2. Boron (a) and silicon (b) powder
Rys. 2. Proszek boru (a) i krzemu (b)

3. Results and discussion

Laser heat treatment with applied laser beam parameters was performed to achieve in the malleable iron modified microstructure of its surface layer with very fine-crystalline melted zone (Fig. 3). Such microstructure was typical for laser treatment with remelting. This zone was characterized by very homogenous, especially in comparison to the core, microstructure or the rest of modified zones in the surface layer.



Source: own work / Źródło: opracowanie własne

Fig. 3. The microstructure of the melted zone in the surface layer of malleable iron after laser heat treatment. Etched with nitride acid solution

Rys. 3. Mikrostruktura strefy przetopionej w warstwie wierzchniej żeliwa ciągliwego po laserowej obróbce cieplnej Trawione nitałem

The graphite phase was rather entirely diluted during the melting. Consequently, the matrix was enriched with carbon. Thus, mainly grains of martensite enriched with alloyed elements and with carbon could be expected in this zone as a result of remelting and mixing of the base micro-

structure (pearlite and graphite) with the substance of alloying elements and rapidly cooled.

Under the melted zone in the malleable iron (as in case in other gray irons: flake or nodular [7]) transition zone was noticed (Figs. 4 and 5). The microstructure of the transition zone consisted of martensite and ledeburite areas. Graphite was almost completely dissolved, that saturated the matrix with carbon during laser heating. It caused (locally) decrease in melting temperature. Thus, as consequence, local melting appeared and ledeburite was formed.



Source: own work / Źródło: opracowanie własne

Fig. 4. The microstructure of the transition zone in the surface layer of malleable iron after laser heat treatment. Etched with nitride acid solution

Rys. 4. Mikrostruktura strefy przejściowej w warstwie wierzchniej żeliwa ciągliwego po laserowej obróbce cieplnej. Trawione nitałem

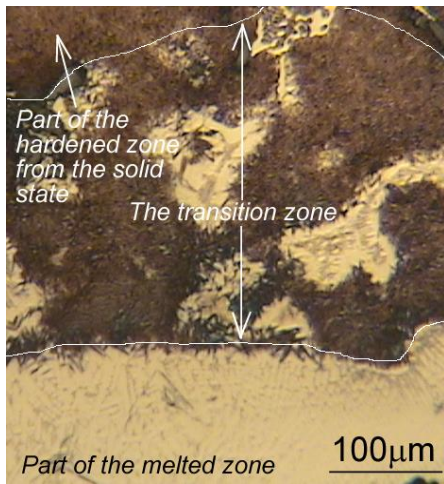


Source: own work / Źródło: opracowanie własne

Fig. 5. The microstructure of the transition zone between the melted zone and the hardened zone from the solid state in the surface layer of malleable iron after laser heat treatment. Etched with nitride acid solution

Rys. 5. Mikrostruktura strefy przejściowej zawartej pomiędzy strefą przetopioną a strefą zahartowaną ze stanu stałego w warstwie wierzchniej żeliwa ciągliwego po laserowej obróbce cieplnej. Trawione nitałem

Nevertheless, as opposed to flake and nodular irons, this zone was found as extremely expanded (Fig. 6). It could be due to more irregular distribution and shape of graphite phase which is characteristic for malleable iron. This base microstructure of malleable iron might be also the reason of larger areas of ledeburite than in case of flake or nodular irons. Such situation (the existence of such an extended transition zone containing the phases that have melted as well as those that have not melted) should favor a particularly good bond between the melted zone and the unmelted base.



Source: own work / Źródło: opracowanie własne

Fig. 6. The microstructure of the cross section through the transition zone, hardened zone from the solid state to core material in the surface layer of malleable iron after laser heat treatment. Etched with nitride acid solution

Rys. 6. Mikrostruktura na przekroju przez strefę przejściową, zahartowaną ze stanu stałego do materiału rdzenia zawartej w warstwie wierzchniej żeliwa ciągliwego po laserowej obróbce cieplnej. Trawione nitałem

Lower than the transition zone, the hardened zone from the solid state (already mentioned) was observed (Fig. 7). This zone was an area in which only martensite and graphite could be distinguished (so without any remelted phases).

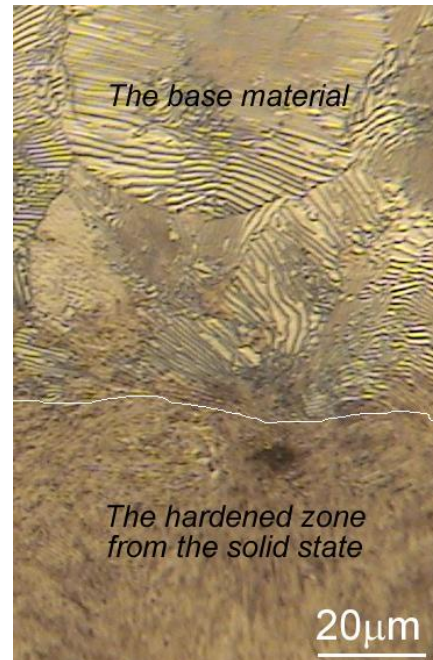


Source: own work / Źródło: opracowanie własne

Fig. 7. The microstructure of the cross section through the transition zone, hardened zone from the solid state to core material in the surface layer of malleable iron after laser heat treatment. Etched with nitride acid solution

Rys. 7. Mikrostruktura na przekroju przez strefę przejściową, zahartowaną ze stanu stałego do materiału rdzenia zawartej w warstwie wierzchniej żeliwa ciągliwego po laserowej obróbce cieplnej. Trawione nitałem

The hardened zone from the solid state was bordered with the core material (consisting of pearlite and graphite – Fig. 1). Between the hardened zone from the solid state and the core material in the case of analyzed cast iron a clear boundary between them could be noticed (Fig. 8).



Source: own work / Źródło: opracowanie własne

Fig. 8. The microstructure of the border between the hardened zone from the solid state and the core material in the surface layer of malleable iron after laser heat treatment. Etched with nitride acid solution

Rys. 8. Mikrostruktura granicy pomiędzy strefą zahartowaną ze stanu stałego a materiałem rdzenia w warstwie wierzchniej żeliwa ciągliwego po laserowej obróbce cieplnej. Trawione nitałem

The changes of the hardness value measured from the surface to the core material after laser heat treatment of the malleable iron was shown in Fig. 9. An almost 4-fold increase (in average) of the melted zone hardness (over 1000HV0.1) was obtained in comparison to the hardness of the matrix of the base material. It is worth to mention, that this zone was the alloyed zone. Thus, this increase was not only because of very fine and hardened microstructure, but also due to supersaturation with alloying elements: boron and silicon.

Not so large scatter of the hardness ($1/2L0.1=51$) confirmed homogenous microstructure of the melted zone visible in the Fig. 3 (as opposed to the transition zone and the hardened zone from the solid state). In case of those zones decrease of the hardness was noticed from approx. 1000HV0.1 to the hardness of the matrix of the core material (about 270HV0.1). It is also worth noting that this cast iron was characterized by high value of the hardness just under the melted zone (reaching approx. 900-1000HV0.1 in its vicinity). It was due to ledeburite existence. The depth of the hardened zone from the solid state (together with the transition zone) was similar to the depth of melted zone. This fact and the gentle hardness changes on the cross section though these zones (from the melted zone to the core material) should cause gentle changes of the internal stresses and favor the wear resistance increase of the malleable iron machine parts treated in this way.

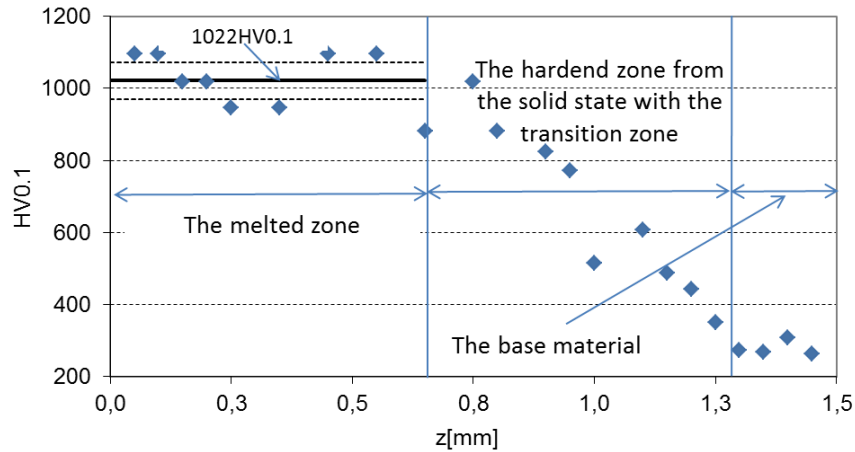


Fig. 9. The changes in the hardness measured from the surface to the core material after laser heat treatment of the malleable iron
Rys. 9. Zmiana twardości zmierzonej od powierzchni w kierunku rdzenia materiału po laserowej obróbce cieplnej żeliwa ciągliwego

The depth of the melted zone was approximately 0.7 mm. Taking in to account that melting for cast irons starts at $\sim 1150^{\circ}\text{C}$ (according to the Fe-C diagram) such depth corresponds to the counted depth (Fig. 10) on the base of equation no 4 (presented in the Methodology). In the Fig. 10 the temperature changes from the treated surface to the core material were presented. Except the temperature changes of EN-GJMB-450-6 malleable iron, also some other gray irons were presented. It could be noticed the specificity of analyzed malleable iron. Its thermophysical properties different from properties of the majority of gray irons cause different effect in its surface layer after laser heat treatment. These proprieties have a crucial influence on the LHT effects in the surface layer. It can be expected (for the same laser heat treatment conditions) a smaller depth of modified layer for malleable iron than the depth for flake irons (for example EN GJL-150, EN GJL-250 or EN GJL-300) and much smaller than the depth for nodular irons (from EN GJS-350 to EN GJS-800) (Fig. 10). Consequently, higher laser beam power density and/or its longer interaction time on the treated surface need to apply in case of malleable iron to attain the similar depth of modified layer after laser treatment as in case of other gray irons.

Another crucial aspect that needs to be taken in to account is related to the cooling rate during laser heat treatment. This part of any heat treatment has the essential influence on the microstructure and, as a result, properties of treated material. In Fig. 11 the evaluated change of the cooling rate value (on the base of equation no 5 presented in the Methodology) from the surface to the core material during the laser heat treatment with the same laser heat treatment conditions (and for the same examples of gray irons as in case of temperature changes - the Fig. 9) was shown. The evaluated cooling rate on the treated surface of malleable iron was lower in approx. $100^{\circ}\text{C}\cdot\text{s}^{-1}$ than for nodular irons. Therefore, it could be expected other conditions of creating microstructure of melted zone in case of analyzed cast iron. Less metastable phases, less supersaturation of solid states could be expected in the surface layer of the malleable iron than for others gray irons (especially nodular) after laser treatment performed in the same conditions. Thus, this is additional important aspect that has to be considered during the selection of the laser heat treatment conditions, especially the values of the laser beam parameters (laser beam power density and its interaction time/scanning velocity).

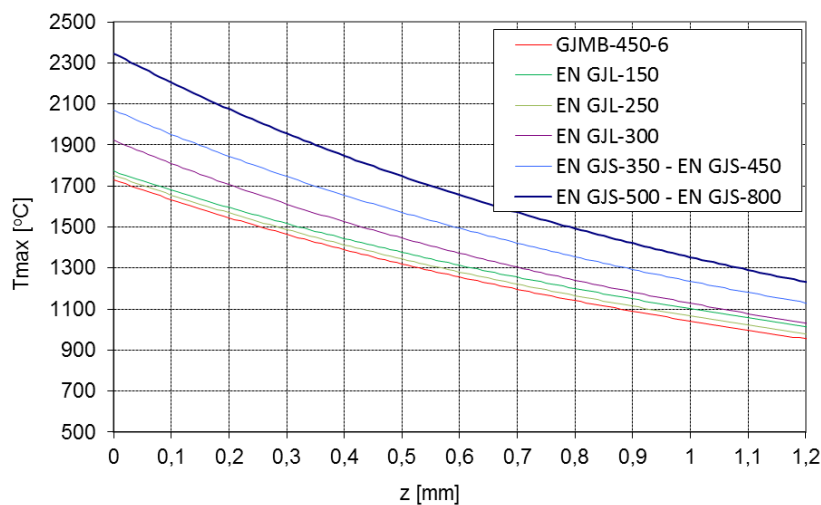


Fig. 10. The evaluated change in the temperature value from the surface to the core material during the laser heat treatment with laser beam power density $E = 26 \text{ W}\cdot\text{mm}^{-2}$ and its scanning velocity $V = 1.87 \text{ mm}\cdot\text{s}^{-1}$ for chosen gray irons
Rys. 10. Oszacowana zmiana wartości temperatury od powierzchni w kierunku rdzenia materiału podczas laserowej obróbki cieplnej z zastosowaniem gęstości mocy wiązki laserowej $E = 26 \text{ W}\cdot\text{mm}^{-2}$ i prędkości jej posuwu $V = 1.87 \text{ mm}\cdot\text{s}^{-1}$ dla wybranych żeliw szarych

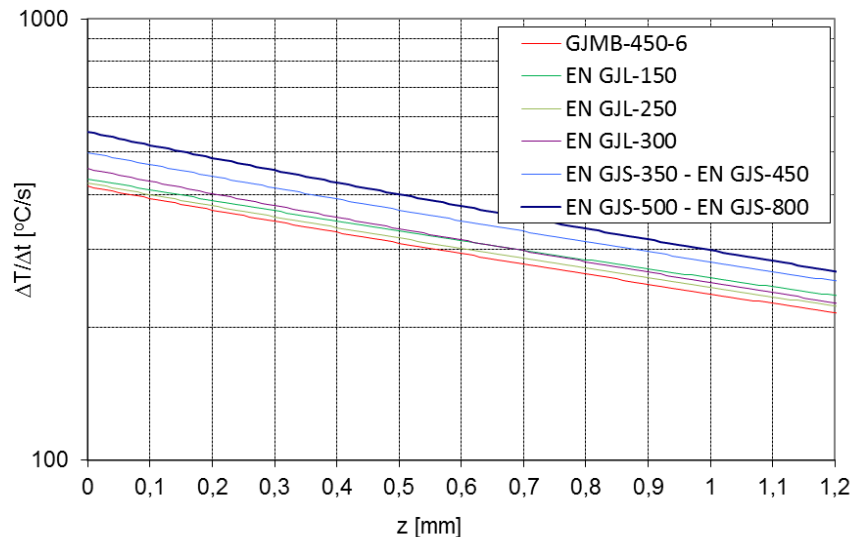


Fig. 11. The evaluated change of the cooling velocity value from the surface to the core material during the laser heat treatment with laser beam power density $E = 26 \text{ W} \cdot \text{mm}^{-2}$ and its scanning velocity $V = 1.87 \text{ mm} \cdot \text{s}^{-1}$ for chosen gray irons

Rys. 11. Oszacowana zmiana wartości prędkości chłodzenia od powierzchni w kierunku rdzenia materiału podczas laserowej obróbki cieplnej z zastosowaniem gęstości mocy wiązki laserowej $E = 26 \text{ W} \cdot \text{mm}^{-2}$ i prędkości jej posuwu $V = 1.87 \text{ mm} \cdot \text{s}^{-1}$ dla wybranych żeliw szarych

The malleable iron, because of its interesting mechanical properties applies in many industry branches. But, in case of the need of the surface treatment by laser heating to machine parts made of this cast iron its special thermophysical properties need to be taken into account.

4. Conclusion

The following conclusions can be formulated on the base of the performed study.

After laser heat treatment of the malleable iron modified microstructure of its surface layer with very fine-crystalline, homogenous and hard (above 1000HV0.1) melted zone was achieved. 4-fold increase in hardness (in comparison to the hardness of matrix of the core material) of melted zone was not only caused by very fine and hardened microstructure, but also due to supersaturating with alloying elements: boron and silicon. The graphite phase was almost entirely diluted during the melting, so the matrix enriched not only with alloyed elements but also with carbon. Under the melted zone transition zone was noticed with martensite and large ledeburite areas. Graphite was also almost completely dissolved. In comparison to flake or nodular irons, this zone was found as extremely expanded. It could be due to more irregular distribution and shape of graphite phase which is characteristic for malleable iron. This base microstructure of malleable iron might be also the reason of larger areas of ledeburite than in case of flake or nodular irons. The existence of such an extended transition zone should favor a good bond between the melted zone and the unmelted base. Below the transition zone the hardened zone from the solid state with martensite and graphite was observed. A very clear boundary between the hardened zone from the solid state and the core material was noticed.

Analyzed cast iron was characterized also by high value of the hardness just under the melted zone (reaching approx. 900-1000HV0.1 in its vicinity). It was due to ledeburite areas existence. The gentle hardness changes (from 1000 to about 270HV0.1) on the cross section though tran-

sition zone and hardened zone from the solid state was noticed. This fact should cause also gentle changes in the internal stresses and favor the wear resistance increase of the malleable iron machine parts treated in this way. Additionally, the depth of the hardened zone from the solid state (together with the transition zone) was similar to the depth of melted zone ($\sim 0.7 \text{ mm}$). Achieved depth of the melted zone corresponded to the counted depth.

Because of some differences in thermophysical properties values between the malleable iron and other gray irons (flake and nodular) the comparison of expected effects of LHT was performed. It allowed to state that for the same laser heat treatment conditions, due to malleable iron properties, a smaller depth of modified layer can be achieved than the depth for flake irons (for example EN GJL-150, EN GJL-250 or EN GJL-300) and much smaller than the depth for nodular irons (from EN GJS-350 to EN GJS-800). It means that higher laser beam power density and/or its longer interaction time on the treated surface need to be applied in case of malleable iron to reach the comparable depth of modified layer after laser treatment as in case of other gray irons. Additionally, the evaluated cooling rate during the laser heat treatment from the surface to the core material also allows to expect differences in the microstructure of the surface layer in the malleable iron than in other gray (particularly nodular) irons. The cooling rate during the laser treatment on the heated surface of malleable iron is lower in approx. $100^\circ\text{C} \cdot \text{s}^{-1}$ than for nodular irons. Less metastable phases, less supersaturation of solid states can be expected in the surface layer of the malleable iron than for others gray irons (especially nodular) after laser treatment performed in the same conditions. Thus, this is additional important feature that has to be considered during the selection of the laser heat treatment conditions (especially the values of the laser beam parameters: laser beam power density and its interaction time/scanning velocity).

The malleable iron, because of its interesting mechanical properties is finding application in many industry branches (also in agricultural). The performed research showed that it is possible to achieve high hardness with mi-

crostructure homogeneity of the surface layer, gentle hardness changes on the cross section from the surface to the core material after laser heat treatment (that should favor the wear resistance increase of the cast iron machine part and favor the selection of this kind of treatment). Nevertheless, in case of applying the laser heat treatment to machine parts made of this cast iron its special thermophysical properties need to be taken in to account.

5. References

- [1] Romek D., Ulbrich D., Selech J., Włodarczyk K., Kowalczyk J.: Evaluation of wear of machine parts made of Armox 600, Ramor 500 and S355 steel with the use of the rotating bowl unit. *Research and Applications in Agricultural Engineering*, 2017, 62(2), 93-95.
- [2] Kośmicki Z., Kęska W., Feder S.: Automatyzacja procesów roboczych maszyn rolniczych. *Prace PIMR*, 2000, 45, 1, 61.
- [3] Paczkowska M.: Zastosowanie technologii laserowych do zwiększania odporności na zużycie elementów maszyn. [w:] *Cywilizacja XXI w. – nowe rozwiązania technologiczne*. Wydawnictwo Naukowe Tygiel, Lublin, 2017.
- [4] Sawczuk W., Jüngst M.: Tarcze hamulcowe pojazdów szynowych. *Technika*, 2016, 12, 496-502.
- [5] Łabęcki M., Gościański, M. Pirowski Z., Olszyński J.: Badania laboratoryjne i eksploatacyjne wybranych elementów roboczych maszyn rolniczych pracujących w glebie, wykonanych z nowoczesnych żeliw ADI. Część 1: Badania laboratoryjne. *Journal of Research and Applications in Agricultural Engineering*, 2004, 49(4), 35.
- [6] Łabęcki M.: Badania laboratoryjne i eksploatacyjne wybranych elementów roboczych maszyn rolniczych pracujących w glebie, wykonanych z nowoczesnych żeliw ADI. Część 2: Badania eksploatacyjne. *Journal of Research and Applications in Agricultural Engineering*, 2004, 49(4), 41.
- [7] Paczkowska M., Analiza wpływu stopowania laserowego na mikrostrukturę warstwy wierzchniej żeliw szarych. *Inżynieria Materiałowa*, 2015, 3, XXXVI, 138-142.
- [8] Paczkowska M.: The evaluation of the influence of laser treatment parameters on the type of thermal effects in the surface layer microstructure of gray irons. *Optics and Laser Technology*, 2016, 76, 143-148.
- [9] Paczkowska M.: Kształtowanie odporności na zużycie tribologiczne elementów maszyn z żeliwa przez laserową obróbkę cieplną (LOC). Wydawnictwo PP, 2016.
- [10] Ashby M.F., Easterling K.E.: The transformation hardening of steel surface by laser beams - I. Hypoeutectoid Steels. *Acta Metall.*, 1984, 32, 1935-1948.

Acknowledgments

This work was financially supported by State Committee for Scientific Research under research Grant N N504 356237 of 2009–2013.